

Rehman

## Solar Potential Assessment of Facades in an Urban Context: An Algorithm for 2.5D Digital Surface Models

Naveed ur Rehman<sup>1</sup>, Timothy Anderson<sup>1</sup> and Roy Nates<sup>1</sup>

<sup>1</sup>*Department of Mechanical Engineering, Auckland University of Technology,  
Auckland, New Zealand*

*E-mail: [timothy.anderson@aut.ac.nz](mailto:timothy.anderson@aut.ac.nz)*

### Abstract

As urban environments become more complex and built-up there is reduced space on roofs for photovoltaic systems, meaning there is an opportunity to develop façade (wall) integrated photovoltaic systems. However, to facilitate this, there is a need to be able to quantify the solar radiation received by specific building facades. As such, this work examines a method for computing solar energy potential of facades in an urban environment. The potential is presented in terms of the ratio of direct solar energy accumulated on facades when the shadowing effects of buildings are considered, to that of an ideal scenario when these shadowing effects are ignored. In achieving this, the method utilizes several spatial-scaled geo-information models, including a 2.5D Digital Surface Model, and the temporal-scaled solar irradiation model such that it is able to assess the potential in a given period. A unique shadow algorithm is also designed to be easily converted into a computer program in which the time and computer memory required for the assessment is independent of the complexity of a given relief. To illustrate this work, a case study considering a hypothetical building layout and orientation is presented.

### 1. Introduction

When quantifying solar energy potential in urban areas, it is essential to realize that harnessing solar energy effectively requires detailed knowledge about its accessibility at the locations of interest (Rehman and Siddiqui, 2015; Rehman and Siddiqui, 2016). In urban areas, it is unlikely that rooftops and façades of several neighbouring buildings would receive an equal amount of solar energy at the same time due to shadowing and sky blocking obstacles in the surroundings.

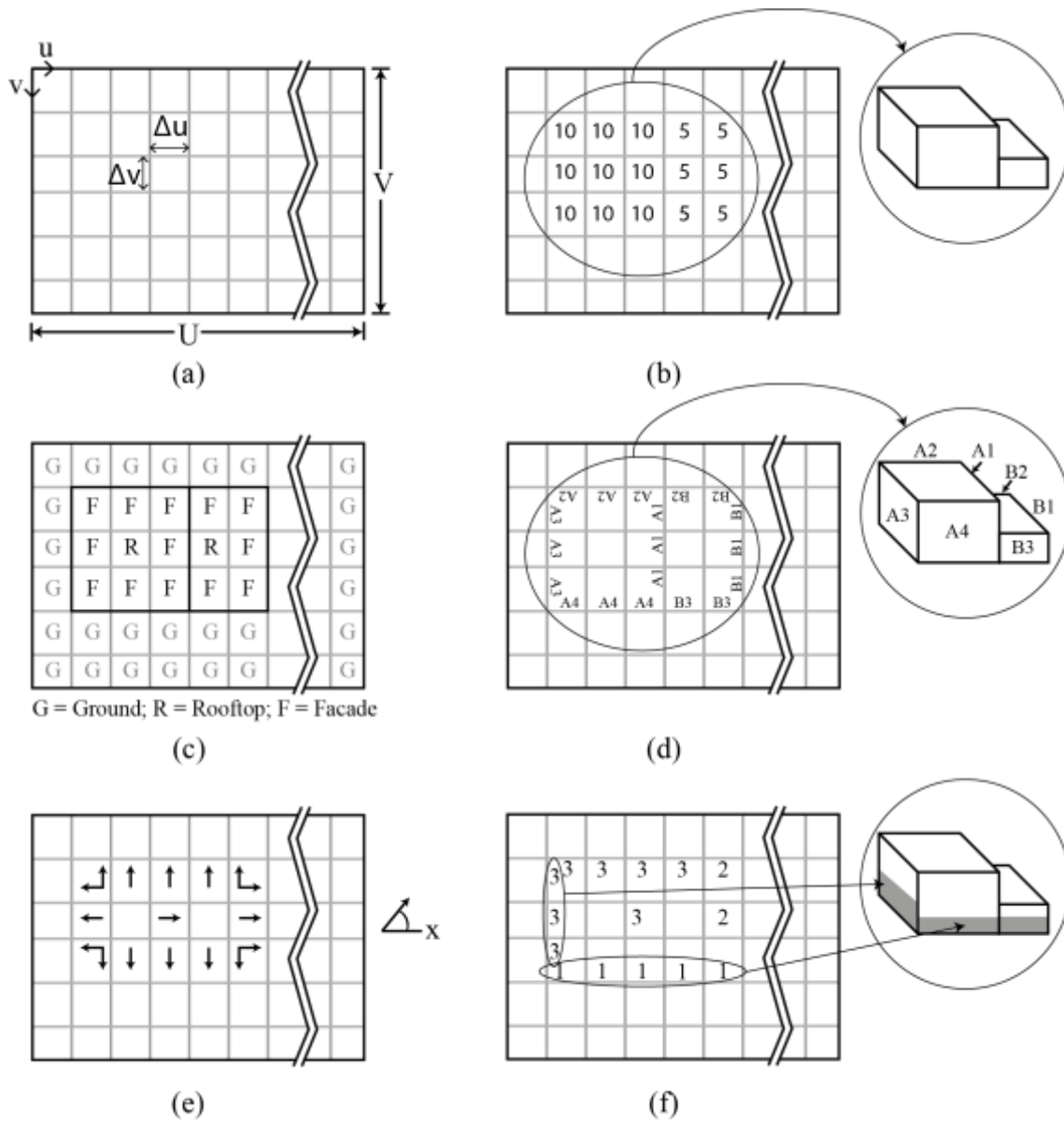
For a viable solar photovoltaic (PV) project, it is crucial that the chosen site should receive sufficiently high solar radiation through the year. To-date, there are several solar potential estimation methodologies and tools available to perform this assessment (Hofierka et al., 2002; Wiginton et al., 2010; Nguyen and Pearce, 2012; Brito et al., 2012; Jakubiec and Reinhart, 2013). These tools make use of geo-information models (GIMs) to obtain urban details such as elevation, surface classification and orientation as well as a solar irradiation model that informs the model of the sun's location in the sky and the magnitude of irradiation at some given instant in time. However, one of the issues with these models is that they have been developed to produce estimates of solar irradiation on horizontal (or moderately inclined) surfaces. In other words, they are not necessarily well suited to yielding estimates on

vertical elements, even when they are adapted for this purpose. One of the main reasons is the inherent characteristic associated with their use of elevation information from Digital Surface Models (DSM) where a façade is represented by only the highest points along its periphery, what is effectively an infinite number of points (called *hyperpoints*). On the other hand deploying solar potential algorithms on exposed surfaces is practically impossible. Even choosing less of these hyperpoints, the considerable number of façades in a typical urban relief will still consume substantial computational resources and time. This may in turn result in highly unrealistic and unreliable estimates (Freitas et al., 2015). In other words, there is a scarcity of methods that can reliably be used to predict solar potential on façades in large and complex urban settings (Carneiro et al., 2010; Redweik et al., 2011; Hofierka and Zlocha, 2012). Hence, developing an approach that is independent of picking hyperpoints for assessing solar potential of façades, yet faster, less memory intensive and reliable would definitely be a significant contribution. As such, this work presents a novel approach to achieving this, along with a compatible shadowing algorithm.

## 2. Methodology

The methodology employs the use of several spatially scaled GIMs and a temporally scaled solar irradiation model (SIM) for estimating the solar potential of façades in an urban relief. The GIM serves as the key input describing the different characteristics of urban features. The generic form of a GIM is a  $\mathbb{R} \times \mathbb{R}$  matrix in which each element has its unique spatial location  $(\mathbb{R}, \mathbb{R})$  and its value denotes the associated characteristics of that location (Figure 1). The range of GIMs used in this study include: the elevation model (Figure 1(b)) which defines the absolute height of the locations (also called a 2.5 DSM), the classification model (Figure 1(c)) which is enumerated according to the class of locations (e.g. ground, roof and façade), the address model (Figure 1(d)) which associates the locations with the feature's address (e.g. building number and façade number), the normal model (Figure 1(e)) which represents the angle of normal to the façade locations (d) and the shadow model (Figure 1(f)) which describes the height of shadow on façades. As the shadow model depends upon the position of the sun in the sky, it will have a temporal dimension as well, i.e. there will be one shadow model for each time step in the analysis.

A typical metrological year (TMY) dataset can be utilized to serve the purpose of the SIM as it contains the hourly information about the position of the sun in the sky, in terms of its altitude  $(\mathbb{R}_\mathbb{R}(\mathbb{R}))$  and azimuth  $(\mathbb{R}_\mathbb{R}(\mathbb{R}))$  angles, and the magnitude of the normal beam irradiation  $(\mathbb{R}_\mathbb{R}(\mathbb{R}), \text{J/m}^2)$ , where  $\mathbb{R}$  represents the hour in local time. In TMY datasets, it is customary that the azimuth angle is measured from true north (positive towards east and negative towards west) and the altitude is measured as positive above the horizon.



**Figure 1. (a) Typical geo-information model (GIM) (b) Elevation Model (c) Classification Model (d) Address Model (e) Normal Model and (f) Shadow Model**

Provided the GIMs and SIM, the hourly radiation ( $\mathcal{Q}(\mathcal{Q}, \mathcal{Q}, \mathcal{Q})$ ,  $J$ ) collected by a vertical element of façade located at  $(\mathcal{Q}, \mathcal{Q})$  during any hour  $\mathcal{Q}$ , can be estimated from Eq. (1):

$$\mathcal{Q}(\mathcal{Q}, \mathcal{Q}, \mathcal{Q}) = \mathcal{Q}_{\mathcal{Q}}(\mathcal{Q}) \cdot [\cos(\mathcal{Q}(\mathcal{Q}, \mathcal{Q}, \mathcal{Q})) \vee 0] \cdot \mathcal{Q}(\mathcal{Q}, \mathcal{Q}) \cdot \mathcal{Q}(\mathcal{Q}, \mathcal{Q}, \mathcal{Q}) \quad (1)$$

where  $\mathcal{Q}(\mathcal{Q}, \mathcal{Q}, \mathcal{Q})$  is the angle of incidence between the directions of the normal to the façade and the normal beam irradiation (Figure 2(a)), the *maximum* operator ‘ $\vee$ ’ discards the radiation “collected” when the sun is behind the collecting surface of façade (i.e.  $90^\circ < \mathcal{Q}(\mathcal{Q}, \mathcal{Q}, \mathcal{Q}) < 270^\circ$ ),  $\mathcal{Q}(\mathcal{Q}, \mathcal{Q})$  (m) and  $\mathcal{Q}(\mathcal{Q}, \mathcal{Q})$  (m) are the width and the unshaded height of the façade, respectively, as shown in Eq. (2):

$$\mathcal{Q}(\mathcal{Q}, \mathcal{Q}, \mathcal{Q}) = \mathcal{Q}(\mathcal{Q}, \mathcal{Q}) - \mathcal{Q}(\mathcal{Q}, \mathcal{Q}, \mathcal{Q}) \quad (2)$$

where  $H(\theta, \phi)$  and  $H_s(\theta, \phi, \phi_s)$  (m) are the total and shaded height of the façade (Figure 2(b)).

The value of angle of incidence can be obtained by the knowledge of the vectors and would be given by Eq. (3):

$$H(\theta, \phi, \phi_s) = \cos^{-1} \left( \frac{\hat{n}(\theta, \phi) \cdot \hat{i}(\phi_s)}{|\hat{n}(\theta, \phi)| |\hat{i}(\phi_s)|} \right) \quad (3)$$

where  $\hat{n}(\theta, \phi)$  and  $\hat{i}(\phi_s)$  are the unit vectors representing the directions of normal to the façade and the normal beam irradiation, respectively (Figure 2 (b) and (c)). These vectors can be written mathematically as Eq. (4) and Eq. (5):

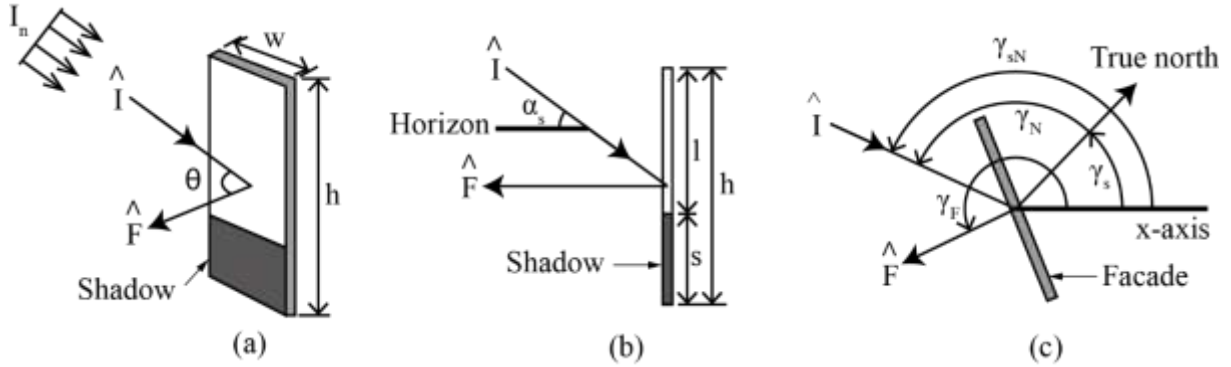
$$\hat{n}(\theta, \phi) = \cos(\phi_p(\theta, \phi)) \hat{n} + \sin(\phi_p(\theta, \phi)) \hat{e} \quad (4)$$

$$\hat{i}(\phi_s) = \cos(\phi_{sp}(\phi_s)) \cos(\phi_s(\phi_s)) \hat{n} + \sin(\phi_{sp}(\phi_s)) \cos(\phi_s(\phi_s)) \hat{e} + \sin(\phi_s(\phi_s)) \hat{e} \quad (5)$$

where  $\phi_p(\theta, \phi)$  is the azimuthal angle of normal to the façade which should be obtain from the normal model and  $\phi_{sp}$  is the azimuthal position of sun, measured CCW from x-axis that can be determined by Eq. (6):

$$\phi_{sp}(\phi_s) = \phi_s(\phi_s) + \phi_p \quad (6)$$

where  $\phi_p$  is the angle of true north measured CCW from x-axis.



**Figure 2. (a) A faade element receiving solar radiation (b) Side-view showing altitudinal angles (c) Top-view showing azimuthal angles**

While the  $H(\theta, \phi)$  can be obtained from elevation model, the calculation of  $H_s(\theta, \phi, \phi_s)$  requires the use of a shadow algorithm. The shadow algorithm proposed here breaks down the elevation model matrix into ' $\phi_{sp}(\phi_s)$ ' number of vectors, each along the unique lines-of-scan ( $\phi_{sp}(\phi_s)$ ) which are parallel to the  $\phi_{sp}(\phi_s)$ . Then, analysing along the  $\phi_{sp}(\phi_s)$ , the height of the shadow on each faade element can be obtained by Eq. (7) (Rehman et al., 2016):

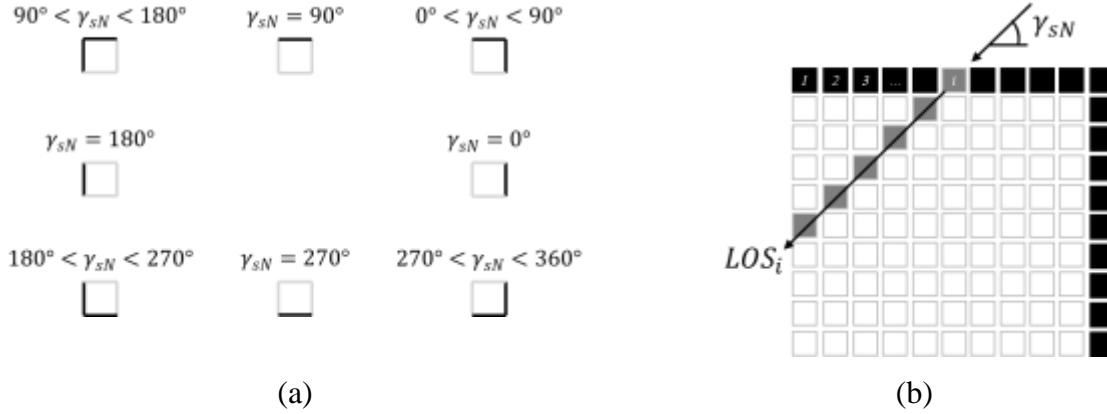
$$H_s(\theta, \phi, \phi_s) = [H(\theta', \phi')] \vee [(H', \phi') - H(\theta) \cdot \tan(\phi_p(\theta))] \quad (7)$$

where  $H(\theta)$  is the distance between the present ( $\theta, \phi$ ) and the preceding element ( $\theta', \phi'$ ) in  $\phi_{sp}(\phi_s)$ , as shown by Eq. (8):

$$H(\theta) = \sqrt{(\theta - \theta')^2 + (\phi - \phi')^2} \quad (8)$$

Note that the element is actually a faade element that is confirmed by the classification model. Extracting the  $\phi_{sp}(\phi_s)$  vectors from elevation model is a two-step procedure. At first,

the initial boundaries of the elevation model are selected according to  $\gamma_{sN}(\theta)$  (Figure 3(a)). The count of the elements in these boundaries represents the total number of vectors. Then, for each element  $\theta$  on the boundary, a vector  $\vec{LOS}_i(\theta)$  is generated by picking and storing the elements of the elevation model, starting from the boundary, to the last element in elevation model, along the direction  $\gamma_{sN}(\theta)$  (Figure 3(b)). The height of shadow at every façade element is finally stored in the  $\theta$ -dimension of shadow model.



**Figure 3. (a) Selecting the initial boundaries in elevation model (b) Extracting line-of-scan vectors from elevation model**

The energy collection over the total time span ( $\theta(\theta, \theta)$ ,  $J$ ) would therefore be obtained from Eq. (9):

$$\theta(\theta, \theta) = \sum_{\theta} \theta(\theta, \theta, \theta) \quad (9)$$

Finally, the address model is referred for compiling the radiation information for each façade address ( $\theta$ ), could be obtained by Eq. (10):

$$\theta(\theta) = \sum \theta(\theta \in \theta, \theta \in \theta) \quad (10)$$

In turn, the maximum radiation collection at the façade locations in the event that there were no shadows would be obtained by Eq. (11)

$$\theta'(\theta, \theta, \theta) = \theta_{\theta}(\theta) \cdot [\cos(\theta(\theta, \theta, \theta)) \vee 0] \cdot \theta(\theta, \theta) \cdot \theta(\theta, \theta) \quad (11)$$

Analogous to Eq. (10),  $\theta'(\theta)$  would represent the maximum solar radiation that could be collected at the façade addresses ( $\theta$ ).

As such, the ratio of Eq. (10) to  $\theta'(\theta)$  represents the measure of the façades solar energy potential, given by Eq. (12):

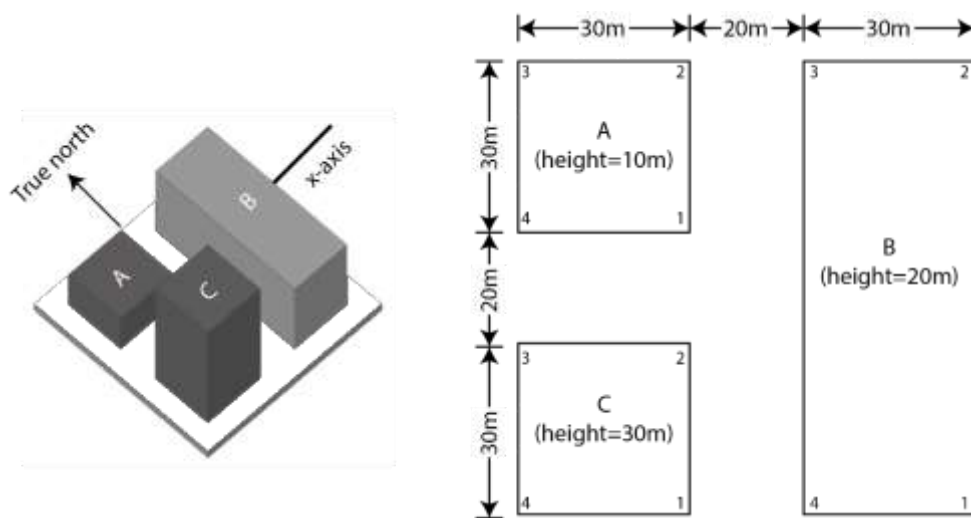
$$\theta(\theta) = \frac{\theta(\theta)}{\theta'(\theta)} \quad (12)$$

Whereas, the potential of an entire urban relief, would be determined from Eq. (13):

$$\theta = \frac{\sum_{\theta} \theta(\theta)}{\sum_{\theta} \theta'(\theta)} \quad (13)$$

### 3. Results and Discussion





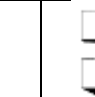





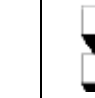

To demonstrate the proposed method a hypothetical layout located in Auckland was chosen for analysis, as shown in Figure 4. The scene consists of three buildings (A, B and C) of different heights, each having four facades and where the angle between the x-axis and true north is  $\theta = 90^\circ$ . The TMY dataset for Auckland obtained from TRNSYS was used as the SIM, from this dataset it was observed that the yearly fractions of the direct normal irradiation approaching from north, south, east and west directions were 88.45%, 11.54%, 47.96% and 52.03% ( $\approx 4814 \text{ MJ/m}^2$ ), respectively.



**Figure 4. Hypothetical layout put up for the simulation and analysis purposes**

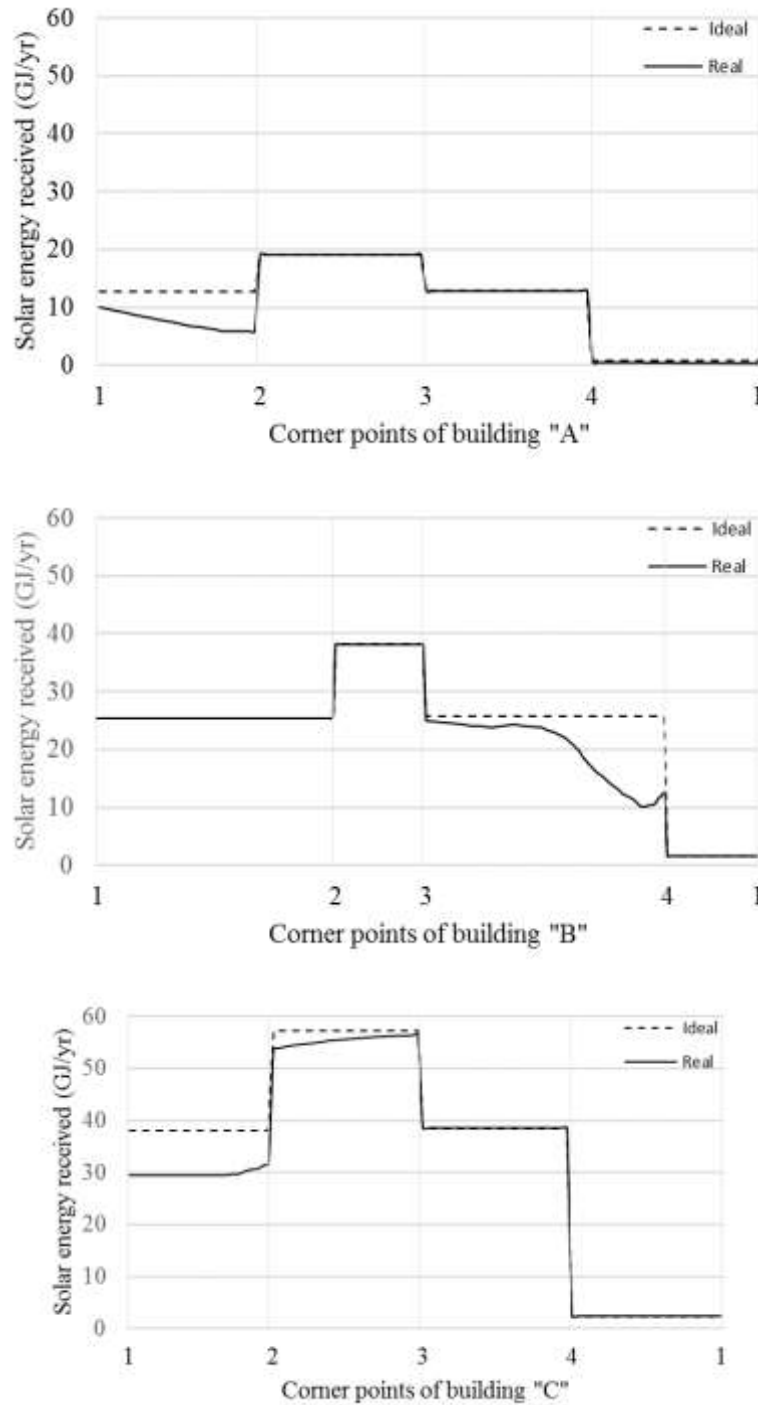
In order to reach a balanced compromise between accuracy of results and computation time, a resolution of  $\Delta\theta = \Delta\tau = 1^\circ$  was chosen when developing GIMs for the layout. Computer codes based on the shadow algorithm proposed in this work were developed for generating the 3696 hourly shadow models. As an example, the shadow models for the different times of the two different days of year (20<sup>th</sup> January and 20<sup>th</sup> June) are shown in Table I.

**Table I. Projected shadows for a typical summer and winter day**

Days\Time	Sunrise	9:00am	12:00pm	Solar noon	3:00pm	Sunset
20 <sup>th</sup> January						
20 <sup>th</sup> June						

The simulations were performed for two different scenarios; in the first scenario, the shadows of the buildings were ignored. This may be called as an “ideal” scenario because the façades received the maximum possible energy. In the second scenario, the shadows cast by the three buildings were taken into consideration; hence, this scenario was a “real” scenario. Figure 5 shows the comparison of façade energy collection in both the scenarios. It can be seen that the

interior façades (i.e. the façades in the layout facing the façades of other building: A-1-2, A-4-1, B-3-4, C-1-2 and C-2-3) receive less energy in the real scenario than in the ideal scenario. The reason for these deviations is obviously the effect of shadows from neighbouring buildings that minimizes the collection at different intervals.



**Figure 5. Solar energy received at the façade locations of buildings**

Table II further summarizes the performance of each façade in the layout. From this, it can be seen that in the ideal scenario the irradiation on the façades, facing the same cardinal direction, is identical. However, in the real scenario, the irradiation at the interior façades is lower due to the shadows of the neighbouring buildings, which reduces the energy collection at several times in a year. Moreover, the façades facing north were found to be receiving the highest solar irradiation ( $1.91 \text{ MJ/m}^2$ ), following the west and east facing façades ( $1.23 - 1.28 \text{ MJ/m}^2$ ).

**Table II. Year-round performance of façades**

Facade				Ideal		Real		Potential
Building	Address	Type	Facing	MJ	MJ/m <sup>2</sup>	MJ	MJ/m <sup>2</sup>	
A	1-2	Interior	East	369	1.23	217	0.72	58.8%
A	2-3	Exterior	North	573	1.91	573	1.91	100.0%
A	3-4	Exterior	West	385	1.28	385	1.28	100.0%
A	4-1	Exterior	South	24	0.08	14	0.05	58.3%
B	1-2	Exterior	East	1968	1.23	1968	1.23	100.0%
B	2-3	Exterior	North	1146	1.91	1146	1.91	100.0%
B	3-4	Interior	West	2054	1.28	1602	1.00	78.0%
B	4-1	Exterior	South	48	0.08	48	0.08	100.0%
C	1-2	Interior	East	1106	1.23	861	1.23	77.8%
C	2-3	Interior	North	1719	1.91	1661	1.91	96.6%
C	3-4	Exterior	West	1155	1.28	1155	1.28	100.0%
C	4-1	Exterior	South	72	0.08	72	0.08	100.0%

Eventually, the yearly collection on all the façades, for the ideal and real scenario, are found to be 10.66 GJ/year and 9.74 GJ/year, respectively. In other words, the solar potential of the layout was found to be 91.36%.

#### 4. Conclusion

A novel hyperpoint-independent approach for estimating solar energy potential of façades in an urban context has been proposed and demonstrated. The solar energy accumulation was determined for each of the façade considering the ideal and real scenarios. It was found that the exterior façades of buildings, facing the same cardinal direction, receives the identical radiation. However, the interior façades receives less radiation due to the shadows of the buildings over each another. This work provides obvious insights to urban planners considering the future potential for façade integrated PV power systems.

#### References

Brito, M., Gomes, N., Santos, T. and Tenedrio, J, 2012, 'Photovoltaic potential in a Lisbon suburb using LiDAR data' *Solar Energy*, 86(1), p283-288.





- Carneiro, C., Morello, E., Desthieux, G. and Golay, F, 2010, 'Urban environment quality indicators: application to solar radiation and morphological analysis on built area' *Proceedings of the 3<sup>rd</sup> WSEAS international conference on visualization, imaging and simulation*, p141-148.
- Freitas, S., Catita, C., Redweik, P. and Brito, M, 2015, 'Modelling solar potential in the urban environment: State-of-the-art review' *Renewable and Sustainable Energy Reviews*, 41, p915-931.
- Hofierka, J. and Zlocha, M, 2012, 'A New 3-D Solar Radiation Model for 3-D City Models' *Transactions in GIS*, 16(5), p681-690.
- Hofierka, J. and Suri, M, 2002, 'The solar radiation model for Open source GIS: implementation and applications' *Proceedings of the Open source GIS-GRASS users conference*, p51-70.
- Jakubiec, J. A. and Reinhart, C. F, 2013, 'A method for predicting city-wide electricity gains from photovoltaic panels based on LiDAR and GIS data combined with hourly Daysim simulations' *Solar Energy*, 93, p127-143.
- Nguyen, H. T. and Pearce, J. M, 2012, 'Incorporating shading losses in solar photovoltaic potential assessment at the municipal scale' *Solar Energy*, 86(5), p1245-1260.
- Redweik, P., Catita, C., Brito, M., and Grande, C, 2011, 'PV potential estimation using 3D local scale solar radiation model based on urban LIDAR data' *Proceedings of the 26<sup>th</sup> European Photovoltaic Solar Energy Conference, Hamburg, Germany*, p5-9.
- Rehman, N. U., and Siddiqui, M. A, 2015, 'A novel method for determining sky view factor for isotropic diffuse radiations for a collector in obstacles-free or urban sites' *Journal of Renewable and Sustainable Energy*, 7(3), 033110.
- Rehman, N. U., and Siddiqui, M. A, 2016, 'A novel methodology for determining sky blocking by obstacles viewed virtually from any location on site' *Energy and Buildings*, 128, p827-833.
- Rehman, N. U., Anderson, T. and Nates, R, 2016, 'Solar Potential Assessment of Facades in an Urban Context: An Algorithm for 1.5D Digital Surface Models' *Asia-Pacific Solar Research Conference, Canberra*, p1-8.
- University of Wisconsin, 2010, 'TRNSYS 17: A transient system simulation program' *Solar Energy Laboratory*.
- Wiginton, L., Nguyen, H., and Pearce, J, 2010, 'Quantifying rooftop solar photovoltaic potential for regional renewable energy policy' *Computers, Environment and Urban Systems*, 34(4), p345-357.